Nanoscale

Dynamic Article Links

Cite this: *Nanoscale*, 2011, **3**, 1504

www.rsc.org/nanoscale

COMMUNICATION

From stochastic single atomic switch to nanoscale resistive memory device†

Attila Geresdi,* András Halbritter, András Gyenis, Péter Makk and György Mihály

Received 6th December 2010, Accepted 21st February 2011
DOI: 10.1039/c0nr00951b

We study the switching characteristics of nanoscale junctions created between a tungsten tip and a silver film covered by a thin ionic conductor layer. Atomic-sized junctions show spectacular current induced switching characteristics, but both the magnitude of the switching voltage and the direction of the switching vary randomly for different junctions. In contrast, somewhat larger junctions with diameters of a few nanometres display a well defined, reproducible switching behavior attributed to the formation and destruction of nanoscale channels in the ionic conductor surface layer. Our results define a lower size limit of 3 nm for reliable ionic nano-switches, which is well below the resolution of recent lithographic techniques.

Solid state ionic conductors are good candidates for the next generation of nonvolatile computer memory elements.[1–5] Such devices have to show reproducible resistance switching at reasonable voltage and current values even if scaled down to nanometre sizes. Solid state memory blocks based on resistive switching have already proven to operate down to the lateral resolution of 100 nm–1 μm (ref. 1, 4, 6, 7, 8). A further decrease of the size, down to the ultimate limit of the single atomic diameter,[9] raises many technical challenges including reproducibility, which is a basic requirement for mass-scale production.[2,10] In such atomic-scale devices the possible junction configurations are determined by the atomic granularity of matter and the fine details of interatomic interactions. The transport through these nanostructures with dimensions comparable to the Fermi wavelength is governed by the quantum nature of conductance: the current is carried along discrete conductance channels. The conductance of a junction is described by the Landauer formula:[11] $G = G_0 \sum_i \tau_i$, the universal conductance quantum $G_0 = 2e^2/h \approx (12.9k\Omega)^{-1}$ being multiplied by the sum of the channel transmission probabilities determined by the details of the junction geometry and the electronic structure of the material.[12]

In this work we study the resistive switching phenomenon on variable size nanoscale junctions with diameters below few tens of nanometres. Variable size point contacts were created by gently touching an Ag thin film sample with an electrochemically sharpened W tip. To enhance the stability of the system, the junctions were created and the measurements were performed at liquid He temperature. More details on the experimental techniques are given in the supplementary material.†

In order to statistically characterize the junctions over a broad scale of diameters we acquired $\approx 10^4$ I–V curves by creating contacts with different conductance values (1 G_0–400 G_0). The diameters of the junctions, estimated by the Sharvin expression,[13] vary from single atom size to $\approx$10 nm.

In this regime the I–V curves regularly exhibit a clear reversible switching behavior in the voltage range of 0.1–1 V (more than 60% of the junctions have shown jumps with relative amplitudes above 10%). Fig. 1 shows typical I–V characteristics for contacts of various conductances. Both the current and voltage values seem to be surprisingly high for a device with dimensions of a few nanometres. The corresponding current densities exceed 10^9 A cm^{-2}. Note, however, that in this mesoscopic transport regime the contacts are

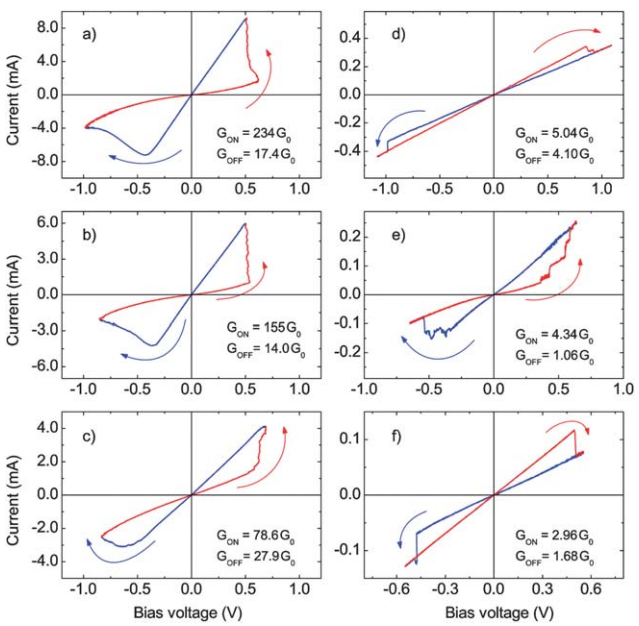

Fig. 1 Resistive switching phenomena for various selected point contacts with different conductance values. The corresponding on- and off-state conductance values measured at $V = 0.1$ V are shown on each graph, respectively. The voltage bias is regarded as positive (negative) if the Ag sample is positively (negatively) biased with respect to the W tip.

Department of Physics, Budapest University of Technology and Economics and Condensed Matter Research Group of the Hungarian Academy of Sciences, 1111 Budapest, Budafoki út 8, Hungary. E-mail: geresdi.attila@wigner.bme.hu

† Electronic supplementary information (ESI) available: Sample characterization, experimental techniques and details on calculations. See DOI: 10.1039/c0nr00951b

not destroyed by the Joule heat, as the dissipation occurs inside a much larger volume determined by the inelastic scattering length.[14,15]

A careful comparison of the curves shown in Fig. 1 reveals significant differences between the characteristics of the junctions with typical on-state conductance of $G_{ON} = 50$–$300\ G_0$ (panels on the left) and that of the smaller contacts with on-state conductance below about $G_{ON} = 20\ G_0$ (panels on the right). Junctions in the first, higher conductance regime will be denoted as *nanoscale junctions*. For such contacts, the current steeply increases as soon as a critical voltage is exceeded. The conductance, however, does not saturate at a predefined value; it increases as long as the applied voltage is ramped up. In our system a serial resistance of $R_s = 90\ \Omega$ is present, which limits this process as the junction's resistance becomes comparable to R_s. Note that in this regime the circuit is not purely voltage driven, which accounts for the back-turning of the *I–V* curve in Fig. 1(a). We found, that in these nanoscale junctions the direction of the current–voltage loops is the same for all the curves.

In contrast, smaller junctions with $G_{ON} < 20\ G_0$—denoted as *atomic-sized contacts*—exhibit a switching behavior between different well defined initial and final states. During the switching event the system jumps to a new state, corresponding to a new line in the *I–V* characteristics, and stays there both for increasing and decreasing voltage ramps (until a back-switching occurs for reversed voltage). The switching voltage, however, scatters in a broad range. Moreover, the direction of the loops is random.

The above features, presented on selected curves, are confirmed by statistical analysis of a large number of junctions. In Fig. 2(a) the switching voltage values are shown in the form of a 2D color scale plot. It is evident that for nanoscale junctions ($G_{ON} > 50\ G_0$) the switching voltage has a relatively well defined value at both polarities around 0.5 V, whereas for atomic-sized contacts ($G_{ON} < 20\ G_0$) the switching voltage scatters randomly in a broad voltage region. An even more obvious distinction is observed in the *direction* of the switching. This is represented by a +1/−1 value if the bias voltage of the sample is positive/negative with respect to the tip for the off → on transition. Averaging the direction of the switching for various junctions with similar conductance, one finds that the switching is always positive for $G_{ON} > 50\ G_0$, whereas for $G_{ON} < 20\ G_0$ the sign of the switching varies randomly (Fig. 2(c)). We argue that the two distinguished switching mechanisms are related to fundamentally different physical phenomena. First we discuss the reproducible resistive switching observed in highly conducting contacts, and later we return to the random switching observed at the atomic level.

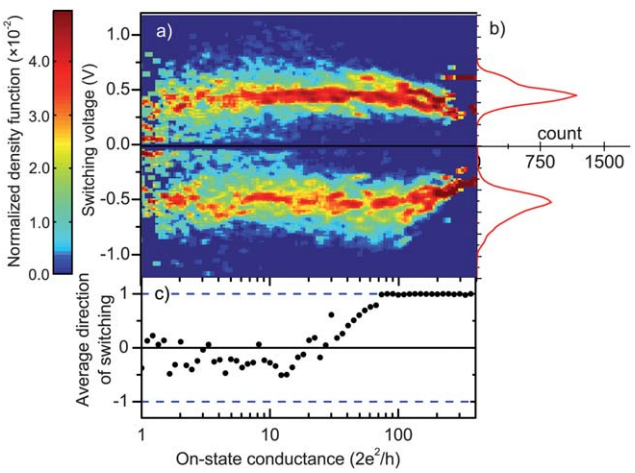

Fig. 2 (a) Switching voltage density plot for *I–V* curves of different on-state conductance values between 1 G_0 and 300 G_0. Color scale represents the relative occurrence of switching threshold voltage as a function of G_{ON}. (b) Switching voltage histograms for curves with $G_{ON} > 50\ G_0$. (c) The averaged switching direction as a function of G_{ON}. +1/−1 represents well defined direction described in the text, while 0 means random direction.

The curves recorded for nanoscale junctions are very similar to those recently reported for resistive switches based on Ag–Ag_2S–Me sandwich structures,[1,16–18] where Me is a transition metal and Ag_2S is an ionic conductor layer formed between the two electrodes. The operation of these devices is based on the electrochemical reaction $Ag^+_{(Ag_2S)} + e^- \rightleftharpoons Ag_{(metal)}$, that is, the solubility of Ag^+ ions in the Ag_2S lattice allows migration controlled by the bias voltage applied. For asymmetric contacts, reversible metallic filaments are built-up and destructed by applying a negative/positive voltage, respectively, which is reflected by abrupt changes in the device conductance. The ionic migration is an activated process[18] resulting in a threshold voltage bias. In our measurements the sign of the switching, the value of the threshold voltage and the overall shape of the curves are consistent with earlier experimental[1,16–18] and theoretical[19] reports on such ionic switches. We emphasize, however, that in our measurements no special treatment of the sample was performed, exposing the Ag layer to air for more than one week was enough to establish the ionic-type switching behavior. More details on sample characterization are provided in the supplementary material.†

In order to demonstrate the universal and reproducible nature of this phenomenon we scaled the individual *I–V* curves recorded in the range from 50 G_0 to 400 G_0 by normalizing them to fixed $G_{OFF} = 1$ and $G_{ON} = 2$ zero bias conductance values. The resulting color density map—acquired from more than 3500 independent *I–V* curves—is shown in Fig. 3, demonstrating that the character of the *I–V* curve is very similar for a broad variety of nanoscale junctions. It is notable that the branch of lower conductance exhibits more pronounced nonlinearity compared to the upper one indicating the tunneling nature[20] of the low-conducting state, which is shunted when metallic filaments are formed. This distinction is even more clearly

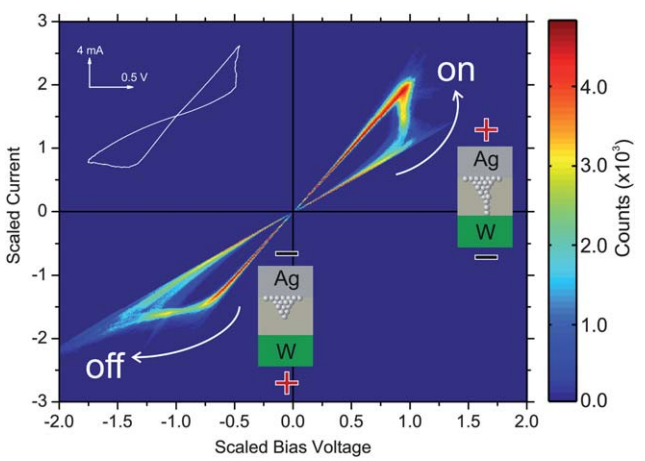

Fig. 3 Color density plot of 3500 independent *I–V* curves normalized to fixed zero bias conductance values. Details of the scaling are given in the supplementary material.† The color scale represents the probability of the scaled *I–V* values. The inset shows a typical switching characteristic.

visible in Fig. 1(a), (b) and (c). The different characters of the on → off and off → on transitions also show clear similarities to the results of earlier measurements.[4,17,21]

It was also studied how the states of the ionic switch can be tuned by the applied bias voltage. Fig. 4(a) demonstrates that *both* states can be altered considerably. For this particular junction, the onset of the resistive switching is at 0.45 V. By gradually increasing the amplitude of the voltage ramp the on and off state resistance values are rapidly tuned. The larger the resistance ratio, the larger the threshold is observed for the off → on transition, which we attribute to a wider insulating gap formed between the metallic sample and the tip.

We found that for constant amplitude ramping the switching phenomenon shows excellent reproducibility and no apparent change is observed for more than 100 cycles, as shown in Fig. 4(b). This stability and reproducibility is characteristic of the ionic switching. Decreasing the contact diameter below about 3 nm, however, results in a crossover to a fundamentally different switching phenomenon.

In the case of the atomic-sized contacts the qualitative observations, especially the random switching sign and the broad range of the threshold voltages, contradict the picture of ionic switching. In this regime we attribute the switching process to atomic rearrangements in the junction due to electromigration induced by the high current density. The relevance of single atomic displacements is demonstrated in Fig. 5(a) and (b), where typical switching traces are presented as conductance-voltage curves. Since the conductance value of a single Ag atom corresponds to the conductance quantum, 1 G_0 (ref. 15), jumps of this magnitude indicate the inclusion or removal of a single atom in the junction area. Multiple steps are often observed with amplitudes close to the integer multiplies of G_0, further supporting this scheme.

The role of the single atomic migration is also supported by the statistical analysis of a large number of switching characteristics. A histogram was made of the conductance traces detected during the voltage sweeps by subtracting the baseline conductance measured in a narrow window (50 mV) around zero bias. The result is shown in

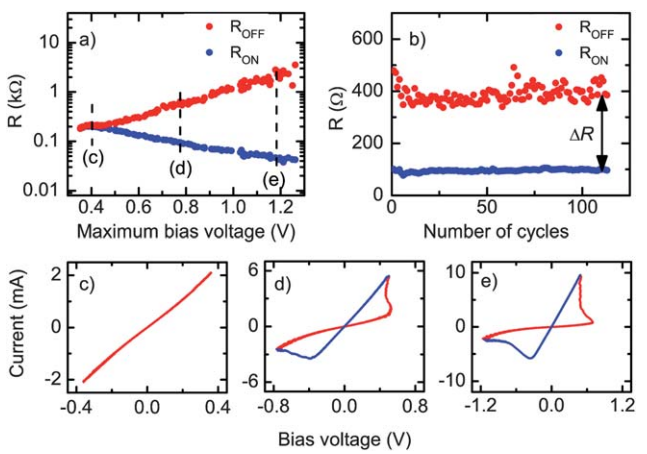

Fig. 4 (a) The evolution of the on- and off-state zero bias conductances as a function of the amplitude of the voltage ramp for a nanoscale ionic switch. Panels (c, d, e) show the *I–V* curves at three different bias voltage amplitudes indicated in panel (a). Panel (b) shows the on- and off-state conductances of a switching device during 100 repeated cycles with a constant amplitude of 0.75 *V* of the voltage ramp. All of these measurements were performed on the same junction.

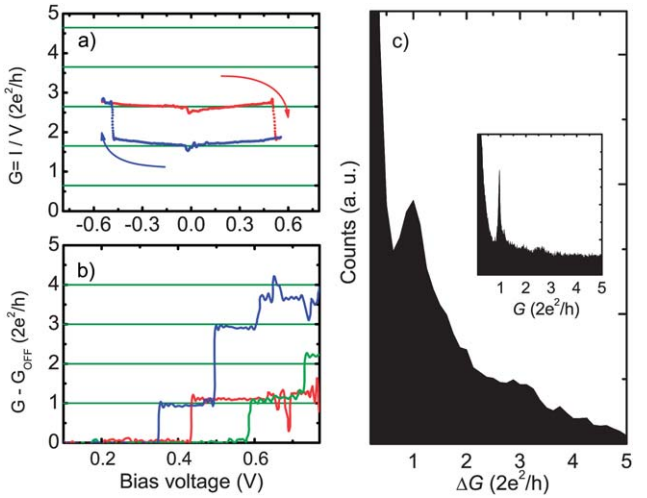

Fig. 5 (a) Conductance *versus* bias voltage curve indicating atomic-scale conductance switching. Green lines are guides to the eye showing a periodicity with $\Delta G = 1\ G_0$ starting from the low-conductance state. (b) Details of the off → on switching for three independent conductance *versus* bias voltage curves with the off-state conductance subtracted. (c) Histogram of the conductance change during the voltage sweep. ΔG is calculated with respect to the zero bias value of the conductance. The histogram is created for 130 independent *I–V* curves with $G_{ON} < 10\ G_0$. The inset shows the histogram of the conductance *versus* electrode separation curves recorded during 5000 repeated opening and closing cycles at a constant bias voltage of 100 mV.

Fig. 5(c). The well defined peak around 1 G_0 reflects that relative jumps corresponding to single atom conductance are dominating. For comparison, the inset shows the traditional conductance histogram measured on the same sample by repeatedly opening and closing the junction with the piezo actuator while monitoring the conductance at a constant bias voltage of 100 mV.

In a control experiment the above phenomenon was investigated in the same voltage and current ranges utilizing the mechanically controllable break junction technique (MCBJ), where the junction is created by the *in situ* breaking of a silver wire.[15] The freshly broken surfaces created in cryogenic vacuum warrant the absence of ionic contamination in the junction. This method fully reproduced the main features of the switching characteristics observed for atomic scale contacts [Fig. 1(d)–(f)], while those of larger junctions were not observed. Preliminary results obtained by the MCBJ technique on pure Au, Pt, Fe revealed that the current induced atomic switching is a quite general phenomenon in atomic-sized junctions.

In conclusion, we have identified two resistive switching mechanisms at the nanoscale. It was shown that the ionic conductor-based devices are good candidates for nonvolatile memory cells as they exhibit stable and reproducible switching behavior. It was demonstrated that solely the exposure of an Ag thin layer to air is enough to establish an ionic conductor surface layer, which is sufficient to form a reliable switching device in a nanoscale point-contact geometry. Our results set a lower limit for the size of such memory cells, below which the character of the switching process dramatically changes due to the enhanced single atomic migration. This size limit is estimated to be $d \approx 3$ nm, resulting in storage densities above the capacity of current NAND flash devices[10] and comparable to the proposed bit size of magnetic media determined by the superparamagnetic limit.[22]

The authors are grateful to L. Bujdosó for sample preparation and to E. Szilágyi for providing the RBS analysis. This work was supported by the New Hungary Development Plan under project ID: TÁMOP-4.2.1/B-09/1/KMR-2010-0002 and by the Hungarian Research Funds OTKA under grants No. 72916 and No. 76010. A. H. is a grantee of the Bolyai János scholarship.

References

1 K. Terabe, T. Hasegawa, T. Nakayama and M. Aono, *Nature*, 2005, **433**, 47–50.
2 S. Kaeriyama, T. Sakamoto, H. Sunamura, M. Mizuno, H. Kawaura, T. Hasegawa, K. Terabe, T. Nakayama and M. Aono, *IEEE J. Solid-State Circuits*, 2005, **40**, 168–176.
3 D. B. Strukov, G. S. Snider, D. R. Stewart and R. S. Williams, *Nature*, 2008, **453**, 80–83.
4 R. Waser and M. Aono, *Nat. Mater.*, 2007, **6**, 833–840.
5 E. Linn, R. Rosezin, C. Kugeler and R. Waser, *Nat. Mater.*, 2010, **9**, 403–406.
6 J. J. Yang, M. D. Pickett, X. Li, Douglas A. A. Ohlberg, D. R. Stewart and R. S. Williams, *Nat. Nanotechnol.*, 2008, **3**, 429–433.
7 S. Dietrich, M. Angerbauer, M. Ivanov, D. Gogl, H. Hoenigschmid, M. Kund, C. Liaw, M. Markert, R. Symanczyk, L. Altimime, S. Bournat and G. Mueller, *IEEE J. Solid-State Circuits*, 2007, **42**, 839–845.
8 Y. Dong, G. Yu, M. C. McAlpine, W. Lu and C. M. Lieber, *Nano Lett.*, 2008, **8**, 386–391.
9 S. J. van der Molen and P. Liljeroth, *J. Phys.: Condens. Matter*, 2010, **22**, 133001.
10 M. Kryder and C. S. Kim, *IEEE Trans. Magn.*, 2009, **45**, 3406–3413.
11 R. Landauer, *Philos. Mag.*, 1970, **21**, 863–867.
12 E. Scheer, N. Agraït, J. C. Cuevas, A. L. Yeyati, B. Ludoph, A. Martin-Rodero, G. R. Bollinger, J. M. van Ruitenbeek and C. Urbina, *Nature*, 1998, **394**, 154–157.
13 Y. U. Sharvin, *Sov. Phys. JETP*, 1965, **21**, 655–656.
14 C. Untiedt, G. Rubio Bollinger, S. Vieira and N. Agraït, *Phys. Rev. B: Condens. Matter*, 2000, **62**, 9962–9965.
15 N. Agraït, A. L. Yeyati and J. M. van Ruitenbeek, *Phys. Rep.*, 2003, **377**, 81–279.
16 K. Terabe, T. Nakayama, T. Hasegawa and M. Aono, *Appl. Phys. Lett.*, 2002, **80**, 4009–4011.
17 M. Morales-Masis, S. J. van der Molen, W. T. Fu, M. B. Hesselberth and J. M. van Ruitenbeek, *Nanotechnology*, 2009, **20**, 095710.
18 A. Nayak, T. Tamura, T. Tsuruoka, K. Terabe, S. Hosaka, T. Hasegawa and M. Aono, *J. Phys. Chem. Lett.*, 2010, **1**, 604–608.
19 M. J. Rozenberg, I. H. Inoue and M. J. Sánchez, *Phys. Rev. Lett.*, 2004, **92**, 178302.
20 J. G. Simmons, *J. Appl. Phys.*, 1963, **34**, 1793–1803.
21 M. Morales-Masis, H.-D. Wiemhofer and J. M. van Ruitenbeek, *Nanoscale*, 2010, **2**, 2275–2280.
22 D. Weller, A. Moser, L. Folks, M. Best, W. Lee, M. Toney, M. Schwickert, J.-U. Thiele and M. Doerner, *IEEE Trans. Magn.*, 2000, **36**, 10–15.